

---

---

# Promising Prospects for $^{44}\text{Sc}$ -/ $^{47}\text{Sc}$ -Based Theragnostics: Application of $^{47}\text{Sc}$ for Radionuclide Tumor Therapy in Mice

Cristina Müller<sup>1</sup>, Maruta Bunka<sup>2,3</sup>, Stephanie Haller<sup>1</sup>, Ulli Köster<sup>4</sup>, Viola Groehn<sup>5</sup>, Peter Bernhardt<sup>6,7</sup>, Nicholas van der Meulen<sup>2</sup>, Andreas Türler<sup>2,3</sup>, and Roger Schibli<sup>1,8</sup>

<sup>1</sup>Center for Radiopharmaceutical Sciences ETH-PSI-USZ, Paul Scherrer Institute, Villigen-PSI, Switzerland; <sup>2</sup>Laboratory of Radiochemistry and Environmental Chemistry, Paul Scherrer Institute, Villigen-PSI, Switzerland; <sup>3</sup>Laboratory of Radiochemistry and Environmental Chemistry, Department of Chemistry and Biochemistry University of Bern, Bern, Switzerland; <sup>4</sup>Institut Laue-Langevin, Grenoble, France; <sup>5</sup>Merck and Cie, Schaffhausen, Switzerland; <sup>6</sup>Department of Radiation Physics, The Sahlgrenska Academy, University of Gothenburg, Gothenburg, Sweden; <sup>7</sup>Department of Medical Physics and Medical Bioengineering, Sahlgrenska University Hospital, Gothenburg, Sweden; and <sup>8</sup>Department of Chemistry and Applied Biosciences, ETH Zurich, Zurich, Switzerland

In recent years,  $^{47}\text{Sc}$  has attracted attention because of its favorable decay characteristics (half-life, 3.35 d; average energy, 162 keV;  $E_{\gamma}$ , 159 keV) for therapeutic application and for SPECT imaging. The aim of the present study was to investigate the suitability of  $^{47}\text{Sc}$  for radionuclide therapy in a preclinical setting. For this purpose a novel DOTA-folate conjugate (cm10) with an albumin-binding entity was used. **Methods:**  $^{47}\text{Sc}$  was produced via the  $^{46}\text{Ca}(n,\gamma)^{47}\text{Ca} \xrightarrow{\beta^-} ^{47}\text{Sc}$  nuclear reaction at the high-flux reactor at the Institut Laue-Langevin. Separation of the  $^{47}\text{Sc}$  from the target material was performed by a semi-automated process using extraction chromatography and cation exchange chromatography.  $^{47}\text{Sc}$ -labeled cm10 was tested on folate receptor-positive KB tumor cells in vitro. Biodistribution and SPECT imaging experiments were performed in KB tumor-bearing mice. Radionuclide therapy was conducted with two groups of mice, which received either  $^{47}\text{Sc}$ -cm10 (10 MBq) or only saline. Tumor growth and survival time were compared between the two groups of mice. **Results:** Irradiation of  $^{46}\text{Ca}$  resulted in approximately 1.8 GBq of  $^{47}\text{Sc}$ , which subsequently decayed to  $^{47}\text{Sc}$ . Separation of  $^{47}\text{Sc}$  from  $^{47}\text{Ca}$  was obtained with 80% yield in only 10 min. The  $^{47}\text{Sc}$  was then available in a small volume (~500  $\mu\text{L}$ ) of an ammonium acetate/HCl (pH 4.5) solution suitable for direct radiolabeling.  $^{47}\text{Sc}$ -cm10 was prepared with a radiochemical yield of more than 96% at a specific activity of up to 13 MBq/nmol. In vitro  $^{47}\text{Sc}$ -cm10 showed folate receptor-specific binding and uptake into KB tumor cells. In vivo SPECT/CT images allowed the visualization of accumulated radioactivity in KB tumors and in the kidneys. The therapy study showed a significantly delayed tumor growth in mice, which received  $^{47}\text{Sc}$ -cm10 (10 MBq, 10 Gy) resulting in a more than 50% increase in survival time, compared with untreated control mice. **Conclusion:** With this study, we demonstrated the suitability of using  $^{47}\text{Sc}$  for therapeutic purposes. On the basis of our recent results obtained with  $^{44}\text{Sc}$ -folate, the present work confirms the applicability of  $^{44}\text{Sc}$ / $^{47}\text{Sc}$  as an excellent matched pair of nuclides for PET imaging and radionuclide therapy.

**Key Words:**  $^{47}\text{Sc}$ ; radionuclide therapy; SPECT; folate receptor; folic acid

**J Nucl Med 2014; 55:1658–1664**  
DOI: 10.2967/jnumed.114.141614

**T**he concept of radiotheragnostic applications is based on the employment of nuclides of the same element allowing the use of chemically identical radiopharmaceuticals for both diagnosis and therapy (1). Several matched pairs of radionuclides have been proposed for this purpose (Table 1; Fig. 1). The best established example is iodine, which has been used for several decades in SPECT ( $^{123}\text{I}$ ) and PET ( $^{124}\text{I}$ ) imaging, as well as for  $\beta^-$  radionuclide therapy ( $^{131}\text{I}$ ) (2). In terms of radiometals, yttrium and copper are elements that comprise radionuclides useful for clinical PET imaging ( $^{86}\text{Y}$  and  $^{61/62/64}\text{Cu}$ ) and for targeted  $\beta^-$  radionuclide tumor therapy ( $^{90}\text{Y}/^{64/67}\text{Cu}$ ) (3–6). Terbium nuclides have been proposed recently for PET ( $^{152}\text{Tb}$ ) and SPECT imaging ( $^{155}\text{Tb}$ ) as well as for  $\alpha$  ( $^{149}\text{Tb}$ ) and  $\beta^-$  radionuclide therapy ( $^{161}\text{Tb}$ ); however, these nuclides have not been made available for clinical application yet (7–9).

In terms of radiotheragnostics, scandium, a trivalent rare earth metal, is of particular interest (Fig. 1) (1).  $^{44}\text{Sc}$  has been recently proposed and investigated for PET imaging, because it decays by the emission of positrons (average energy [ $E_{\beta^+}$  average], 632 keV; intensity, 94.3%), with a half-life ( $T_{1/2}$ ) of 3.97 h (10). These properties would potentially allow the distribution of  $^{44}\text{Sc}$ -labeled radiopharmaceuticals to hospitals without cyclotron and radiopharmaceutical laboratories available.

$^{47}\text{Sc}$  was proposed as a potential therapeutic match to the PET nuclide  $^{44}\text{Sc}$ . It is a low-energy  $\beta^-$  emitter with decay characteristics ( $T_{1/2}$ , 3.35 d;  $E_{\beta^-}$ , 162 keV) that are potentially useful for radionuclide tumor therapy similar to the clinically established  $^{177}\text{Lu}$  ( $T_{1/2}$ , 6.65 d;  $E_{\beta^-}$ , 134 keV;  $E_{\gamma}$ , 113, 208 keV). The most obvious difference between  $^{47}\text{Sc}$  and  $^{177}\text{Lu}$  is the significantly shorter half-life of  $^{47}\text{Sc}$ . This characteristic would be particularly favorable for the combination of  $^{47}\text{Sc}$  with small-molecular-weight and peptide-based targeting ligands with a relatively fast blood clearance. Moreover,  $^{47}\text{Sc}$  has been proposed for radioimmunotherapy (11). Under the assumption that it forms stable complexes

---

Received Apr. 14, 2014; revision accepted Jun. 9, 2014.  
For correspondence or reprints contact: Cristina Müller, Center for Radiopharmaceutical Sciences ETH-PSI-USZ, Paul Scherrer Institute, 5232 Villigen-PSI, Switzerland.  
E-mail: cristina.mueller@psi.ch  
Published online Jul. 17, 2014.  
COPYRIGHT © 2014 by the Society of Nuclear Medicine and Molecular Imaging, Inc.

**TABLE 1**  
Nuclear Data of Theragnostic Isotopes for Therapy, PET, and SPECT Imaging

	Therapeutic nuclide			PET nuclide			SPECT nuclide		
	Half-life	$E\beta^-_{av}$ [keV]	$E\gamma$ [keV] (I [%])	Half-life	$E\beta^+_{av}$ [keV] (I [%])		Half-life	$E\gamma$ [keV] (I [%])	
$^{131}\text{I}$	8.02 d	182	364 (82)	$^{124}\text{I}$	4.15 d	820 (22.7)	$^{123}\text{I}$	13.2 h	159 (83)
$^{90}\text{Y}$	2.67 d	933	-	$^{86}\text{Y}$	14.74 h	660 (31.9)			
$^{67}\text{Cu}$	2.58 d	141	91–93 (23) 185 (49)	$^{64}\text{Cu}$	12.7 h	278 (17.6)			
				$^{61}\text{Cu}$	3.33 h	500 (61.0)			
				$^{62}\text{Cu}$	9.67 min	1,319 (97.8)			
$^{161}\text{Tb}$	6.90 d	154	45–53 (39) 75 (10)	$^{152}\text{Tb}$	17.5 h	1,080 (17.0)	$^{155}\text{Tb}$	5.32 d	105 (25) 87 (32)
$^{149}\text{Tb}$	4.1 h	3,970 (a)	165 (26)						
$^{47}\text{Sc}$	3.35 d	162	159 (68)	$^{44}\text{Sc}$	3.92 h	632 (94.3)			

with open-chained chelators (e.g., octadentate diethylene triamine pentaacetic acid) as recently proposed (12), radiolabeling of antibodies would become accessible at room temperature. Similar to  $^{177}\text{Lu}$ , the decay of  $^{47}\text{Sc}$  is also accompanied by the emission of  $\gamma$ -rays of an ideal energy ( $E\gamma$ , 159 keV; intensity, 68.3%) for SPECT imaging. For all of these reasons,  $^{47}\text{Sc}$  is a highly promising new candidate of a radionuclide for potential application in therapeutic nuclear medicine.

The goal of the present study was to investigate  $^{47}\text{Sc}$  as a therapeutic pendant to the recently tested PET nuclide  $^{44}\text{Sc}$  (13) using the same targeting principle. The DOTA-folate conjugate (cm10) used in this study is composed of the same functionalities as was the case for the previously evaluated folate conjugate cm09 (14). Folic acid binds selectively to the folate receptor (FR), which is expressed on a variety of tumor types, including cancer of the ovaries and of the lungs (15,16). The DOTA-chelator can be used for stable coordination of Sc as previously demonstrated (13,17). Finally, there is a small-molecular-weight albumin-binding entity (18) integrated in the folate conjugate cm10. This

additional functionality was shown to enhance the blood circulation time of folate conjugates and, as a consequence, to improve the tissue distribution profile (13). In the present study,  $^{47}\text{Sc}$ -cm10 was evaluated in vitro using FR-positive KB tumor cells and in vivo by the performance of biodistribution and SPECT/CT studies. Radionuclide therapy was conducted with two groups of KB tumor-bearing mice, which received either  $^{47}\text{Sc}$ -cm10 or saline only. The average tumor growth and survival time were compared between treated animals and untreated controls.

## MATERIALS AND METHODS

### Production of $^{47}\text{Sc}$

$^{47}\text{Ca}$  was produced via the  $^{46}\text{Ca}(n,\gamma)^{47}\text{Ca}$  nuclear reaction by irradiation of a  $^{46}\text{Ca}$  target (dried nitrate, 1 mg of metal mass, 31.7% enrichment of  $^{46}\text{Ca}$ ) for 3.94 d in a thermal neutron flux of  $1.5 \times 10^{15} \text{ cm}^{-2}\text{s}^{-1}$  at the high-flux reactor of Institut Laue-Langevin in Grenoble, France.  $^{47}\text{Ca}$  decays to  $^{47}\text{Sc}$ , with a half-life of 4.54 d, by the emission of  $\beta^-$  particles and  $\gamma$ -rays. This allowed repeated chemical separation of the daughter nuclide  $^{47}\text{Sc}$  in a pseudogenerator-like system. For the separation of  $^{47}\text{Sc}(\text{III})$  from  $\text{Ca}(\text{II})$  ( $^{47}\text{Ca}$  and stable calcium isotopes), a previously developed semiautomated separation system was used (13). In brief, the irradiated target was dissolved in HCl (3 M, prepared from 30% HCl, Suprapur [Merck KGaA]) and loaded onto a column containing  $N,N,N',N'$ -tetra-*n*-octyldiglycolamide (DGA, 50–100  $\mu\text{m}$  [Triskem International]) extraction resin. The adsorbed  $^{47}\text{Sc}(\text{III})$  was eluted from the DGA resin with HCl (0.1 M,  $\sim 3 \text{ mL}$ ). The acidic  $^{47}\text{Sc}(\text{III})$  eluate (0.1 M HCl) was loaded onto a second column containing a cation exchange resin in water (DOWEX 50, hydrogen form, 200–400 mesh [Fluka Analytic]).  $^{47}\text{Sc}(\text{III})$  was eluted with a mixture of  $\text{CH}_3\text{COONH}_4$  and HCl (0.75 and 0.2 M, respectively;  $\sim 500 \mu\text{L}$ , pH 4.5;  $\text{CH}_3\text{COONH}_4$ : Trace SELECT,  $\geq 99.9999\%$ , Fluka Analytic; HCl 30%: Suprapur, Merck KGaA).

### Radiosynthesis

The organic synthesis of the albumin-binding DOTA-folate (cm10) is reported in the supplemental data (available at <http://jnm.snmjournals.org>). For the preparation

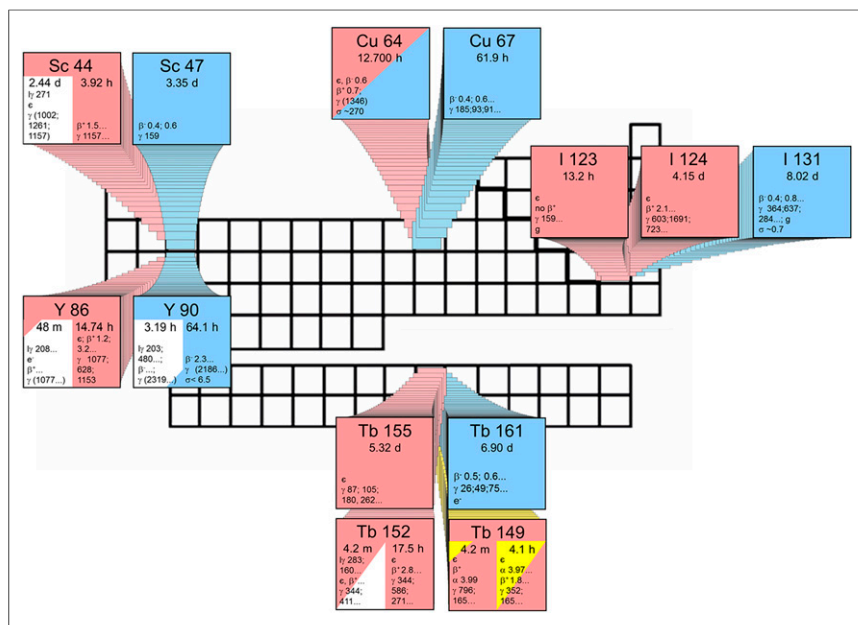


**FIGURE 1.** Theragnostic principle: matched pairs of radionuclides for PET or SPECT imaging and for therapeutic application in nuclear medicine. Radionuclides are designated according to Karlsruhe's Chart of Nuclides.

**TABLE 2**  
Biodistribution of <sup>47</sup>Sc-cm10 in KB Tumor-Bearing Nude Mice

Organ	<sup>47</sup> Sc-cm10 (% injected activity per gram tissue*)						
	1 h after injection	4 h after injection	24 h after injection	48 h after injection	72 h after injection	96 h after injection	168 h after injection
Blood	5.80 ± 1.09	3.33 ± 0.86	0.40 ± 0.08	0.23 ± 0.03	0.15 ± 0.04	0.09 ± 0.04	0.02 ± 0.01
Lung	3.08 ± 0.35	2.30 ± 0.53	0.98 ± 0.15	0.56 ± 0.16	0.57 ± 0.21	0.60 ± 0.22	0.29 ± 0.07
Spleen	1.22 ± 0.12	0.86 ± 0.14	0.47 ± 0.10	0.39 ± 0.05	0.46 ± 0.10	0.51 ± 0.27	0.33 ± 0.16
Kidneys	23.3 ± 2.1	35.4 ± 1.1	28.8 ± 3.9	23.3 ± 3.9	21.2 ± 4.6	18.1 ± 2.1	9.8 ± 2.7
Stomach	1.71 ± 0.16	1.21 ± 0.19	0.44 ± 0.04	0.47 ± 0.05	0.44 ± 0.11	0.44 ± 0.17	0.24 ± 0.08
Intestines	0.83 ± 0.05	0.65 ± 0.12	0.31 ± 0.07	0.26 ± 0.04	0.21 ± 0.07	0.19 ± 0.05	0.10 ± 0.04
Liver	4.44 ± 0.40	4.46 ± 0.83	2.42 ± 0.36	2.15 ± 0.32	1.51 ± 0.22	1.64 ± 0.73	0.68 ± 0.16
Salivary glands	7.47 ± 1.81	7.40 ± 0.97	3.75 ± 0.66	2.90 ± 0.33	2.91 ± 0.65	3.01 ± 0.74	1.51 ± 0.49
Muscle	1.79 ± 0.23	1.14 ± 0.52	0.92 ± 0.18	1.07 ± 0.21	0.72 ± 0.18	0.37 ± 0.11	0.16 ± 0.06
Bone	1.54 ± 0.11	1.09 ± 0.23	0.70 ± 0.16	0.63 ± 0.10	0.63 ± 0.30	0.67 ± 0.29	0.45 ± 0.24
Tumor	9.81 ± 1.24	17.96 ± 2.17	13.82 ± 1.87	12.00 ± 2.34	11.65 ± 1.54	8.31 ± 1.03	4.19 ± 1.50
Tumor-to-blood	1.6 ± 0.4	5.6 ± 1.4	35.8 ± 8.0	52.0 ± 4.7	79.7 ± 17.2	106 ± 45	173 ± 45
Tumor-to-liver	2.1 ± 0.1	4.1 ± 0.6	5.8 ± 1.2	5.6 ± 0.4	7.8 ± 0.3	5.8 ± 2.5	6.4 ± 2.7
Tumor-to-kidney	0.40 ± 0.06	0.51 ± 0.03	0.48 ± 0.02	0.52 ± 0.06	0.56 ± 0.07	0.47 ± 0.09	0.44 ± 0.18

\*Values shown represent mean ± SD of data from 3 animals (*n* = 3) per cohort.

of <sup>47</sup>Sc-cm10, a stock solution of cm10 (10 μL, 10<sup>-3</sup> M) was added to the solution of <sup>47</sup>Sc in CH<sub>3</sub>COONH<sub>4</sub>/HCl (~250 μL; 130 MBq, pH ~4.5) and incubated at 95°C for 10 min. Sodium diethylene triamine pentaacetic acid (5 μL, 5 mM, pH 5) was added to the reaction mixture for the complexation of potential traces of free <sup>47</sup>Sc(III). Quality control was performed by high-performance liquid chromatography. For preclinical application, variable amounts of cm10 were added to obtain the required specific activity. For in vivo application, the labeling mixture containing <sup>47</sup>Sc-cm10 was diluted with 3 parts of an equivalent volume of MilliQ water to reduce the osmolarity (365 mOsm). In vitro stability and cell experiments are reported in the supplemental data.

#### Biodistribution Studies

In vivo experiments were approved by the local veterinarian department and conducted in accordance with the Swiss law of animal protection. Four- to 5-wk-old female athymic nude mice (CD-1 Foxn-1/nu) were purchased from Charles River Laboratories. The animals were fed a folate-deficient rodent diet (ssniff Spezialdiät10 GmbH) starting 5 d before KB tumor cell (5 × 10<sup>6</sup> cells in 100 μL of phosphate-buffered saline) inoculation into the subcutis of each shoulder. Biodistribution studies were performed in triplicate approximately 14 d after cell inoculation. <sup>47</sup>Sc-cm10 (2 MBq, 1 nmol/mouse) was injected in a volume of 100 μL into a lateral tail vein. The animals were sacrificed at pre-determined time points after administration of <sup>47</sup>Sc-cm10. Selected tissues and organs were collected, weighed, and counted for radioactivity using a γ-counter. The results were listed as a percentage of the injected activity per gram of tissue mass (%IA/g), using counts of a defined volume of the original injection solution counted at the same time. Dosimetric calculations were performed on the basis of these data (supplemental data).

#### SPECT Studies

SPECT/CT studies were performed with a 4-head multiplexing multipinhole camera (NanoSPECT/CT; Mediso Medical Imaging Systems). Each head was outfitted with a tungsten-based aperture of nine 1.4-mm-diameter pinholes and a thickness of 10 mm. SPECT/CT images were acquired by use of NuLine software (version 1.02; Bioscan). CT scans were obtained with the integrated CT using a tube voltage of 55 kVp and an exposure time of 1.0 s per view.

After the acquisitions, SPECT data were reconstructed iteratively with HiSPECT software (version 1.4.3049; Scivis GmbH) using the γ-energy of 159 keV ± 10% of <sup>47</sup>Sc. The real-time CT reconstruction used a cone-beam filtered backprojection. SPECT and CT data were automatically co-registered, because both modalities shared the same axis of rotation. The fused datasets were analyzed with the InVivo-Scope postprocessing software (version 1.44; Bioscan Inc.).

In vivo SPECT/CT imaging studies were performed with a nude mouse approximately 14 d after KB tumor cell inoculation. <sup>47</sup>Sc-cm10 (~13 MBq, 1 nmol/mouse) was intravenously injected. For the in vivo scan, the mouse was anesthetized by inhalation of an isoflurane-oxygen mixture. The scans were obtained with a time-per-view of 100–350 s, resulting in a scan time of about 1 h (48 h after injection in vivo) and 4.5 h (96 h after injection post-mortem), respectively. All SPECT scans were preceded by a CT scan.

#### Preclinical Therapy Study Using <sup>47</sup>Sc-cm10

KB cells (4.5 × 10<sup>6</sup> cells in 100 μL of phosphate-buffered saline) were subcutaneously injected 4 d before the start of therapy at day 0. Two groups (groups A and B) consisting of 6 mice each were injected with only saline (group A, control) or with <sup>47</sup>Sc-cm10 (group B, 10 MBq, 1 nmol) at day 0 when the average KB tumor volume reached 53 ± 24 mm<sup>3</sup> in the mice of group A and 61 ± 20 mm<sup>3</sup> in the mice of group B. The mice were weighed 3 times a week over a period of about 7 wk. The relative body weight (RBW) was defined as [BW<sub>x</sub>/BW<sub>0</sub>], where BW<sub>x</sub> is the body weight in grams at a given time *x* and BW<sub>0</sub> the body weight at day 0. The tumor volume was determined by measuring 2 dimensions with a digital caliper and calculated according to the equation [0.5 × (L × W<sup>2</sup>)], where L is the longest axis and W the axis perpendicular to L in millimeters (19). The relative tumor volume (RTV) was defined as [TV<sub>x</sub>/TV<sub>0</sub>], where TV<sub>x</sub> is the tumor volume in mm<sup>3</sup> at a given time *x* and TV<sub>0</sub> the tumor volume at day 0. The efficacy of <sup>47</sup>Sc-cm10-based therapy was expressed as the percentage tumor growth inhibition (TGI), calculated using the equation [100 - (T/C × 100)], where T is the mean RTV of the treated mice and C is the mean RTV in the control group at the time of euthanasia of the first mouse of the control group (20). Tumor growth delay (TGD<sub>x</sub>) was calculated as the time required for the tumor volume to increase *x*-fold over the initial volume at the day 0.

The tumor growth delay index [ $TGDI_x = TGD_x(T)/TGD_x(C)$ ] was calculated as the  $TGD_x$  ratio of treated mice (T) over control mice (C) for a 5-fold ( $x = 5$ ,  $TGD_5$ ) and 10-fold ( $x = 10$ ,  $TGD_{10}$ ) increase of the initial tumor volume.

Endpoint criteria were defined as body weight loss of more than 15% of the initial body weight (at day 0), KB tumor volume more than 1,000 mm<sup>3</sup>, ulceration or bleeding of the tumor xenograft, or abnormal behavior indicating pain or unease of the animal. Mice were removed from the study and euthanized on reaching one of the predefined endpoint criteria. To calculate significance of the survival time and tumor growth delay, a *t* test (Excel software; Microsoft) was used. All analyses were 2-tailed and considered as type 3 (2-sample unequal variance). A *P* value of less than 0.05 was considered statistically significant.

## RESULTS

### Production of <sup>47</sup>Sc

Irradiation of the <sup>46</sup>Ca target (1 mg) for 3.94 d at the high-flux reactor of Institut Laue-Langevin resulted in the production of approximately 1.8 GBq of <sup>47</sup>Ca and approximately 0.6 GBq of <sup>47</sup>Sc at the end of irradiation. After shipment of the target to the Paul Scherrer Institute,  $\gamma$ -ray spectrometry was performed with an aliquot of the dissolved target solution. Apart from <sup>47</sup>Ca ( $E_\gamma$ , 489.2, 807.9, and 1,297.1 keV) and its decay product <sup>47</sup>Sc ( $E_\gamma$ , 159.4 keV), no radionuclidic impurities were detectable (supplemental data).

### Separation of <sup>47</sup>Sc

At the time of the first separation of <sup>47</sup>Sc(III) from carrier-added <sup>47</sup>Ca(II) (5.8 d after end of irradiation), the activity of <sup>47</sup>Sc was approximately 900 MBq. The separation of <sup>47</sup>Sc was performed using extraction chromatography and cation exchange chromatography within approximately 10 min, as previously reported (Fig. 2) (13). A DGA column served for adsorption of <sup>47</sup>Sc from 3 M HCl whereas the <sup>47</sup>Ca remained in solution and was eluted (Fig. 2A). Then, the <sup>47</sup>Sc(III) was eluted with 0.1 M HCl (Fig. 2B). For subsequent concentration of the <sup>47</sup>Sc solution, a DOWEX 50-based cation exchange chromatography column was used. <sup>47</sup>Sc (~740 MBq in ~500  $\mu$ L; first separation) was formulated at a radioactivity concentration of up to approximately 1.5 GBq/mL in a solution (0.75 M NH<sub>4</sub>Ac/0.2 M HCl, pH ~4.5) that was suitable for a direct radiolabeling process (Fig. 2C). A second separation of approximately 240 MBq of <sup>47</sup>Sc was performed 3.9 d later, after renewed generation of <sup>47</sup>Sc (~300 MBq). The overall yield of <sup>47</sup>Sc after separation was approximately 80%, and the amount of

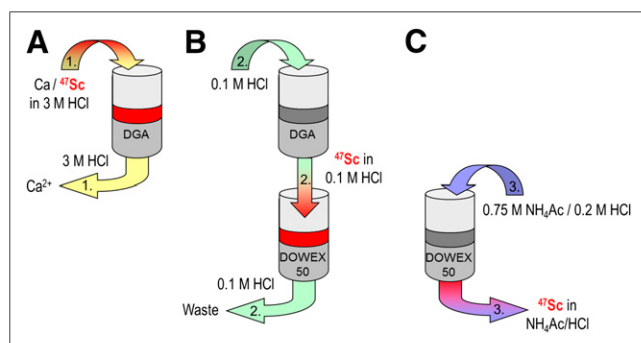


**FIGURE 2.** Separation process of <sup>47</sup>Sc from calcium in 3 steps. (A) Dissolved target is loaded onto column I where <sup>47</sup>Sc is adsorbed and calcium is eluted. (B) <sup>47</sup>Sc is eluted and directly loaded onto column II where it is adsorbed. (C) Elution of <sup>47</sup>Sc from column II.

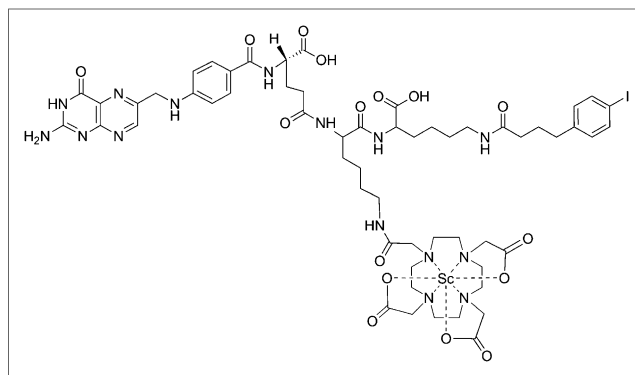


**FIGURE 3.** Chemical structure of <sup>47</sup>Sc-labeled DOTA-folate conjugate (cm10) with speculative coordination sphere of scandium radionuclide.

<sup>47</sup>Ca in the collected <sup>47</sup>Sc fraction was less than 1% (supplemental data).

### Preparation and In Vitro Evaluation of <sup>47</sup>Sc-cm10

The preparation of <sup>47</sup>Sc-cm10 was performed as previously reported (Fig. 3) (13). Quality control performed by high-performance liquid chromatography showed the product peak of <sup>47</sup>Sc-cm10, with a retention time of 19.3 min. The radiochemical yield was more than 96% at a specific activity of up to 13 MBq/nmol, representing a <sup>47</sup>Sc-to-ligand molar ratio of 1:110. <sup>47</sup>Sc-cm10 was stable in phosphate-buffered saline with only minimal release of <sup>47</sup>Sc(III) (<3%) within the first 24 h. Uptake and internalization of <sup>47</sup>Sc-cm10 into KB tumor cells was increasing over time. FR-specific binding was proven by the fact that uptake of <sup>47</sup>Sc-cm10 was reduced to less than 1% in cell samples, which were co-incubated with excess folic acid to block the receptors (Fig. 4).

### Biodistribution Studies

Biodistribution studies with <sup>47</sup>Sc-cm10 showed a high accumulation of radioactivity in the tumor tissue, with a maximum value of  $18.0 \pm 2.2$  %IA/g at 4 h after injection and an excellent retention over time ( $11.7 \pm 1.5$  %IA/g at 72 h after injection) (Table 2). Radioactivity measured in the blood was decreasing rapidly from  $5.8 \pm 1.1$  %IA/g at 1 h after injection to background levels after 1 d ( $0.4 \pm 0.1$  %IA/g). Significant accumulation of radioactivity was also found in the kidneys ( $28.8 \pm 3.9$  %IA/g; 24 h after injection) and in the salivary glands ( $3.8 \pm 0.7$  %IA/g; 24 h after

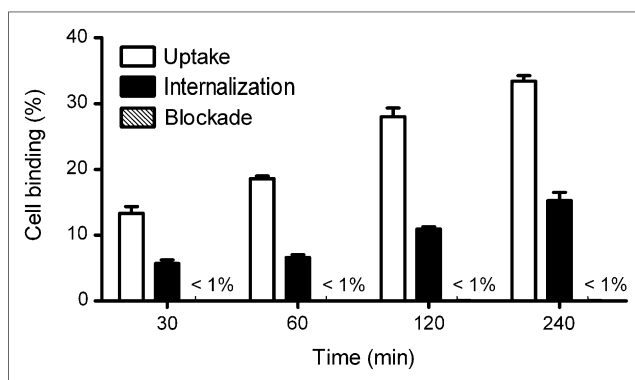


**FIGURE 4.** Time-dependent uptake and internalization of <sup>47</sup>Sc-cm10 in KB cells. Values are indicated as percentage of total added radioactivity per 0.15 mg of protein. Co-incubation with excess folic acid resulted in blocked uptake (<1%) of <sup>47</sup>Sc-cm10.

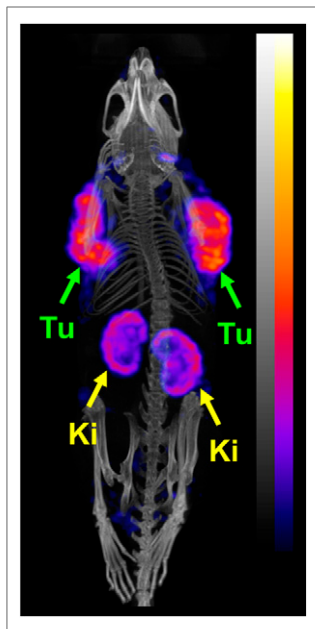


**FIGURE 5.** SPECT/CT image of KB tumor-bearing mouse 48 h after injection of approximately 13 MBq of  $^{47}\text{Sc}$ -cm10. Ki = kidney; Tu = tumor.

injection) where the FR is expressed. In the liver, the uptake was relatively high shortly after the injection of  $^{47}\text{Sc}$ -cm10 ( $4.4 \pm 0.4\%$ IA/g; 1 h after injection) but decreased constantly over time to  $1.6 \pm 0.7\%$ IA/g at 96 h after injection. In all other tissue and organs such as lung, spleen, stomach, intestines, muscle, and bone, retention of radioactivity was low and decreased further over time.

For tumor xenografts and kidneys, the absorbed dose was calculated as approximately 1.0 and 2.0 Gy/MBq, respectively, resulting in an absorbed tumor dose of approximately 10 Gy and a kidney dose of 20 Gy on a single injection of 10 MBq of  $^{47}\text{Sc}$ -cm10.

#### In Vivo SPECT Imaging Studies Using $^{47}\text{Sc}$ -cm10

SPECT/CT studies were performed with a KB tumor-bearing mouse 48 h after injection of  $^{47}\text{Sc}$ -cm10 (Fig. 5), enabling excellent visualization of the tumors, the sites of highest accumulation of radioactivity. Besides, uptake of radioactivity was seen only in the kidneys. This is always observed after injection of folate-based radioconjugates because of their specific binding to FRs expressed in the proximal tubule cells. However, in the liver, lung, spleen, and intestinal tract, radioactivity was not retained.

#### Preclinical Therapy Study Using $^{47}\text{Sc}$ -cm10

In the mice of group A, which received only saline, the KB tumors were growing constantly over time, whereas in the  $^{47}\text{Sc}$ -cm10-treated mice of group B the tumor growth was clearly delayed (Fig. 6A). At day 21 of the study, the first control mouse (group A) had to be euthanized because of an oversized tumor. At that time point, the calculated tumor growth index revealed a value of 73% (Table 3). The tumor growth delay inhibition of treated mice calculated for an RTV of 5 (TGDI<sub>5</sub>) was  $2.0 \pm 0.6$ , indicating a 2-fold increased time for tumors to reach the same volume as the control animals. To

reach an RTV of 10, the required time had increased 1.5-fold in treated animals, compared with untreated control animals, reflected by a TGDI<sub>10</sub> of  $1.5 \pm 0.3$  (Table 3).

After injection of  $^{47}\text{Sc}$ -cm10, the mice experienced slight body weight loss (Fig. 6B). Throughout the investigation, the average RBW of treated mice (group A) was somewhat lower than the RBW of untreated control mice, but extensive body weight loss (>15%) was not observed. The average survival time was 25 d for control mice and 38.5 d for treated mice, which meant an additional survival time of 54% in the case of  $^{47}\text{Sc}$ -cm10 therapy (Fig. 6C).

#### DISCUSSION

In the past,  $^{47}\text{Sc}$  has been proposed as a new radionuclide for application in therapeutic nuclear medicine (11,21). Herein, we reported on the first, to our knowledge, preclinical in vivo study performed with a  $^{47}\text{Sc}$ -labeled small-molecular-weight biomolecule for tumor targeting. In this respect, a novel DOTA-folate conjugate (cm10) was used. In vitro  $^{47}\text{Sc}$ -cm10 showed results comparable to the previously investigated  $^{177}\text{Lu}$ -cm09 (14). In vivo,  $^{47}\text{Sc}$ -cm10 was assessed in biodistribution studies over 7 d using KB tumor-bearing mice. High uptake of  $^{47}\text{Sc}$ -cm10 was found in tumor xenografts and in the kidneys, because both of these tissues express the FR substantially. In the blood and in non-targeted organs and tissues, retention of radioactivity decreased over time, reaching background levels after about 24 h. These data were comparable to, but not completely the same as, those previously obtained with  $^{177}\text{Lu}$ -cm09 (14). Potential reasons for certain discrepancies could be the fact that the experiments with  $^{177}\text{Lu}$ -cm09 and  $^{47}\text{Sc}$ -cm10 were not performed in parallel (inter-experimental variability) and that these radioconjugates differed not only with regard to the used radionuclide ( $^{47}\text{Sc}$  vs.  $^{177}\text{Lu}$ ) but also with regard to the chemical structure of the DOTA-folate conjugate (cm10 vs. cm09). SPECT/CT imaging experiments obtained after injection of  $^{47}\text{Sc}$ -cm10 in KB tumor-bearing mice confirmed the post-mortem tissue distribution data. The images showed also an excellent analogy to the PET scans obtained with mice after injection of  $^{44}\text{Sc}$ -cm10 (supplemental data). Additional SPECT studies were performed with Derenzo phantoms to compare  $^{47}\text{Sc}$  with  $^{177}\text{Lu}$ . The images showed an equally high resolution for both nuclides, confirming the suitability of using  $^{47}\text{Sc}$  for SPECT imaging, which would be important for pre-therapeutic dosimetry in patients (supplemental data).

The most crucial part for the assessment of  $^{47}\text{Sc}$  was the performance of a therapy experiment, which was conducted with the standard KB tumor mouse model according to a protocol previously

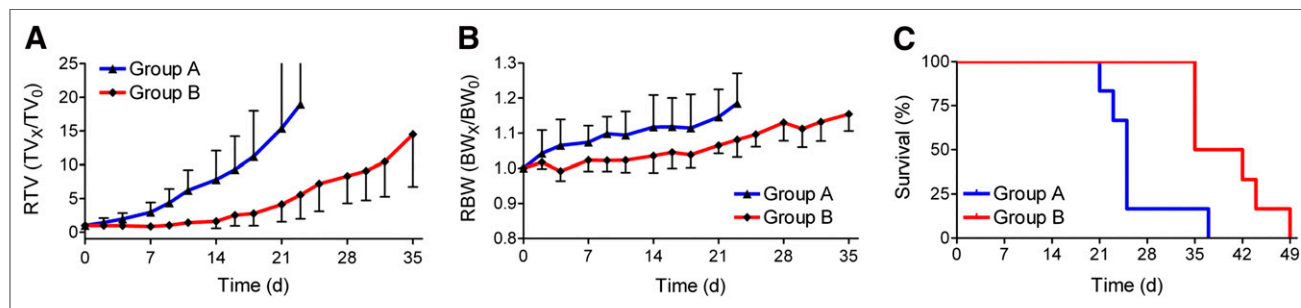


**FIGURE 6.** RTV (A), RBW (B), and survival (C) of mice in preclinical therapy study. Mice of group A received saline, and mice of group B received 10 MBq of  $^{47}\text{Sc}$ -cm10. Average survival time was 25 d (group A) and 38.5 d (group B).

**TABLE 3**  
Results of Therapy Study with  $^{47}\text{Sc}$ -cm10

Group (mice)	$^{47}\text{Sc}$ -cm10	TGDI <sub>5</sub> *	TGDI <sub>10</sub> †	TGI (d 21)	Survival time
A (n = 6)	—	1.0 ± 0.0	1.0 ± 0.0	—	25 d
B (n = 6)	10 MBq	2.0 ± 0.6‡	1.5 ± 0.3*	73% ± 17%	38.5 d (i.e., +54%)

\*TGDI<sub>5</sub> = Tumor growth delay index of mice calculated for RTV of 5.

†TGDI<sub>10</sub> = Tumor growth delay index of mice calculated for RTV of 10.

‡P < 0.05.

used for  $^{177}\text{Lu}$ -cm09 and  $^{161}\text{Tb}$ -cm09 (9). The estimation of the absorbed tumor dose after injection of 10 MBq of  $^{47}\text{Sc}$ -cm10 revealed a value of about 10 Gy. The significant tumor growth delay observed in treated mice resulted in additional survival time (+54%), compared with untreated controls. Despite the much lower tumor dose, the data suggest a comparable antitumor efficacy of  $^{47}\text{Sc}$ -cm10 with the previously evaluated  $^{177}\text{Lu}$ -cm09 (~24 Gy) and  $^{161}\text{Tb}$ -cm09 (~33 Gy) (9) at the same quantity of injected activity (10 MBq/mouse) and in the same tumor mouse model. Because of the limited availability of  $^{47}\text{Sc}$ , kidney toxicity studies have not been performed yet. However, it is likely that renal damage, which has been observed with other therapeutic folate radioconjugates, would be absent at such low dose levels of only 20 Gy to the kidneys. This assumption is based on the commonly used kidney dose limit of approximately 23 Gy, which was found to be safe during external radiation therapy (22). Should the findings of this study be confirmed in further in vivo studies,  $^{47}\text{Sc}$  may be of considerable interest for a clinical application of targeted radionuclide tumor therapy.

In the near future,  $^{47}\text{Sc}$  should be made available at sufficient quantities to allow further and more extended preclinical therapy studies. In the present study, the production of  $^{47}\text{Sc}$  was accomplished via the  $^{46}\text{Ca}(n,\gamma)^{47}\text{Ca} \xrightarrow{\beta^-} ^{47}\text{Sc}$  nuclear reaction. Enriched  $^{46}\text{Ca}$  was irradiated at a high-flux reactor to produce  $^{47}\text{Ca}$ , which, in turn, decays to  $^{47}\text{Sc}$ . The application of such a radionuclide pseudogenerator system provides an opportunity to separate the daughter nuclide  $^{47}\text{Sc}$  from the mother nuclide  $^{47}\text{Ca}$  several times. However, a significant drawback of this production route is the high price of enriched  $^{46}\text{Ca}$  as a result of its extremely low abundance of only 0.004% in natural calcium. Alternative routes for the production of  $^{47}\text{Sc}$  have been reported in the literature (23–26). Among these, the most feasible appears to be the irradiation of  $^{47}\text{Ti}$  targets with fast neutrons to induce the  $^{47}\text{Ti}(n,p)^{47}\text{Sc}$  nuclear reaction (25,27,28). In this respect, more investigations will be necessary to evaluate the production at a larger scale and optimize the isolation conditions of  $^{47}\text{Sc}$ . If this will be successful, application of  $^{47}\text{Sc}$  in preclinical and most likely also clinical studies will be approachable in the future.

## CONCLUSION

In this study, the promising potential of  $^{47}\text{Sc}$  was demonstrated for the first time in combination with a small-molecular-weight targeting agent in a preclinical setting. Excellent features of  $^{47}\text{Sc}$  for application in therapeutic nuclear medicine have been confirmed.  $^{47}\text{Sc}$  is in particular attractive as part of the theragnostic principle together with  $^{44}\text{Sc}$ , which may be used for pre-therapeutic imaging as well as therapy planning and monitoring. In view of these promising future prospects for  $^{47}\text{Sc}$ , further preclinical experiments,

using larger cohorts of animals and variable targeting agents, will be necessary. Moreover, comparison of  $^{47}\text{Sc}$  with the clinically established  $\beta^-$  emitter  $^{177}\text{Lu}$  will be crucial to draw final conclusions about the suitability of  $^{47}\text{Sc}$  for clinical application.

## DISCLOSURE

The costs of publication of this article were defrayed in part by the payment of page charges. Therefore, and solely to indicate this fact, this article is hereby marked “advertisement” in accordance with 18 USC section 1734. The project was financially supported by the Swiss Cancer League (KLS-02762-02-2011). No other potential conflict of interest relevant to this article was reported.

## ACKNOWLEDGMENTS

We thank Dr. Konstantin Zhernosekov for initiating the study and Martin Hungerbühler for technical assistance.

## REFERENCES

- Rösch F, Baum RP. Generator-based PET radiopharmaceuticals for molecular imaging of tumours: on the way to THERANOSTICS. *Dalton Trans.* 2011;40: 6104–6111.
- Lopci E, Chiti A, Castellani MR, et al. Matched pairs dosimetry:  $^{124}\text{I}/^{131}\text{I}$  metaiodobenzylguanidine and  $^{124}\text{I}/^{131}\text{I}$  and  $^{86}\text{Y}/^{90}\text{Y}$  antibodies. *Eur J Nucl Med Mol Imaging.* 2011;38(suppl 1):S28–S40.
- Walrand S, Flux GD, Konijnenberg MW, et al. Dosimetry of yttrium-labelled radiopharmaceuticals for internal therapy:  $^{86}\text{Y}$  or  $^{90}\text{Y}$  imaging? *Eur J Nucl Med Mol Imaging.* 2011;38(suppl 1):S57–S68.
- Anderson CJ, Dehdashti F, Cutler PD, et al.  $^{64}\text{Cu}$ -TETA-octreotide as a PET imaging agent for patients with neuroendocrine tumors. *J Nucl Med.* 2001;42: 213–221.
- Anderson CJ, Ferdani R. Copper-64 radiopharmaceuticals for PET imaging of cancer: advances in preclinical and clinical research. *Cancer Biother Radiopharm.* 2009;24:379–393.
- O'Donnell RT, DeNardo GL, Kukis DL, et al. A clinical trial of radioimmunotherapy with  $^{67}\text{Cu}$ -2IT-BAT-Lym-1 for non-Hodgkin's lymphoma. *J Nucl Med.* 1999;40:2014–2020.
- Lehenberger S, Barkhausen C, Cohrs S, et al. The low-energy beta<sup>-</sup> and electron emitter  $^{161}\text{Tb}$  as an alternative to  $^{177}\text{Lu}$  for targeted radionuclide therapy. *Nucl Med Biol.* 2011;38:917–924.
- Müller C, Zhernosekov K, Köster U, et al. A unique matched quadruplet of terbium radioisotopes for PET and SPECT and for  $\alpha$ - and  $\beta^-$ -radionuclide therapy: an in vivo proof-of-concept study with a new receptor-targeted folate derivative. *J Nucl Med.* 2012;53:1951–1959.
- Müller C, Reber J, Haller S, et al. Direct in vitro and in vivo comparison of  $^{161}\text{Tb}$  and  $^{177}\text{Lu}$  using a tumour-targeting folate conjugate. *Eur J Nucl Med Mol Imaging.* 2014;41:476–485.
- Roesch F. Scandium-44: benefits of a long-lived PET radionuclide available from the  $^{44}\text{Ti}/^{44}\text{Sc}$  generator system. *Curr Radiopharm.* 2012;5:187–201.
- Kolsky KL, Joshi V, Mausner LF, Srivastava SC. Radiochemical purification of no-carrier-added scandium-47 for radioimmunotherapy. *Appl Radiat Isot.* 1998;49:1541–1549.

12. Polosak M, Piotrowska A, Krajewski S, Bilewicz A. Stability of  $^{47}\text{Sc}$ -complexes with acyclic polyamino-polycarboxylate ligands. *J Radioanal Nucl Chem.* 2013;295:1867–1872.
13. Müller C, Bunka M, Reber J, et al. Promises of cyclotron-produced  $^{44}\text{Sc}$  as a diagnostic match for trivalent  $\beta$ -emitters: in vitro and in vivo study of a  $^{44}\text{Sc}$ -DOTA-folate conjugate. *J Nucl Med.* 2013;54:2168–2174.
14. Müller C, Struthers H, Winiger C, Zhernosekov K, Schibli R. DOTA conjugate with an albumin-binding entity enables the first folic acid-targeted  $^{177}\text{Lu}$ -radioisotope tumor therapy in mice. *J Nucl Med.* 2013;54:124–131.
15. Weitman SD, Lark RH, Coney LR, et al. Distribution of the folate receptor GP38 in normal and malignant cell lines and tissues. *Cancer Res.* 1992;52:3396–3401.
16. Parker N, Turk MJ, Westrick E, Lewis JD, Low PS, Leamon CP. Folate receptor expression in carcinomas and normal tissues determined by a quantitative radioligand binding assay. *Anal Biochem.* 2005;338:284–293.
17. Majkowska-Pilip A, Bilewicz A. Macrocyclic complexes of scandium radionuclides as precursors for diagnostic and therapeutic radiopharmaceuticals. *J Inorg Biochem.* 2011;105:313–320.
18. Dumelin CE, Trüssel S, Buller F, et al. A portable albumin binder from a DNA-encoded chemical library. *Angew Chem Int Ed Engl.* 2008;47:3196–3201.
19. Reddy JA, Westrick E, Santhapuram HK, et al. Folate receptor-specific antitumor activity of EC131, a folate-maytansinoid conjugate. *Cancer Res.* 2007;67:6376–6382.
20. Sancéau J, Poupon MF, Delattre O, Sastre-Garau X, Wietzerbin J. Strong inhibition of Ewing tumor xenograft growth by combination of human interferon-alpha or interferon-beta with ifosfamide. *Oncogene.* 2002;21:7700–7709.
21. Srivastava SC, Mausner LF, Mease RC. Criteria for the selection of radionuclides for tumor radioimmunotherapy. IAEA INIS website. [http://www.iaea.org/inis/collection/NCLCollectionStore/\\_Public/23/010/23010630.pdf](http://www.iaea.org/inis/collection/NCLCollectionStore/_Public/23/010/23010630.pdf). Accessed July 3, 2014.
22. Emami B, Lyman J, Brown A, et al. Tolerance of normal tissue to therapeutic irradiation. *Int J Radiat Oncol Biol Phys.* 1991;21:109–122.
23. Yagi M, Kondo K. Preparation of carrier-free  $^{47}\text{Sc}$  by  $^{48}\text{Ti}$  ( $\gamma, p$ ) reaction. *Int J Appl Radiat Isot.* 1977;28:463–468.
24. Kopecky P, Szelecsenyi F, Molnar T, Mikecz P, Tarkanyi F. Excitation-functions of ( $p, xn$ ) reactions on  $^{48}\text{Ti}$ -monitoring of bombarding proton-beams. *Appl Radiat Isot.* 1993;44:687–692.
25. Mausner LF, Kolsky KL, Joshi V, Srivastava SC. Radionuclide development at BNL for nuclear medicine therapy. *Appl Radiat Isot.* 1998;49:285–294.
26. Habs D, Köster U. Production of medical radioisotopes with high specific activity in photonuclear reactions with gamma-beams of high intensity and large brilliance. *Appl Phys B.* 2011;103:501–519.
27. Bokhari TH, Mushtaq A, Khan IU. Separation of no-carrier-added radioactive scandium from neutron irradiated titanium. *J Radioanal Nucl Chem.* 2010;283:389–393.
28. Bartos B, Majkowska A, Kasperk A, Krajewski S, Bilewicz A. New separation method of no-carrier-added  $^{47}\text{Sc}$  from titanium targets. *Radiochim Acta.* 2012;100:457–461.